Theory uncertainties in the fiducial Drell–Yan cross section and distributions

Xuan Chen[1,2], Thomas Gehrmann[3], Nigel Glover[4], Alexander Huss[5], Pier Francesco Monni[5], Emanuele Re[6,7], Luca Rottoli[3†], Paolo Torrielli[8]

[1] *Institute for Theoretical Physics, Karlsruhe Institute of Technology, 76131 Karlsruhe, Germany*
[2] *Institute for Astroparticle Physics, Karlsruhe Institute of Technology, 76344 Eggenstein-Leopoldshafen, Germany*
[3] *Department of Physics, University of Zürich, CH-8057 Zürich, Switzerland*
[4] *Institute for Particle Physics Phenomenology, Physics Department, Durham University, Durham DH1 3LE, UK*
[5] *CERN, Theoretical Physics Department, CH-1211 Geneva 23, Switzerland*
[6] *Dipartimento di Fisica G. Occhialini, U2, Università degli Studi di Milano-Bicocca and INFN, Sezione di Milano-Bicocca, Piazza della Scienza, 3, 20126 Milano, Italy*
[7] *LAPTh, Université Grenoble Alpes, Université Savoie Mont Blanc, CNRS, F-74940 Annecy, France*
[8] *Dipartimento di Fisica and Arnold-Regge Center, Università di Torino and INFN, Sezione di Torino, Via P. Giuria 1, I-10125, Turin, Italy*

In these proceedings we study various sources of theoretical uncertainty in the Drell–Yan $p_T^{\ell\ell}$ spectrum focussing on the $p_T^{\ell\ell} \lesssim 100\,\text{GeV}$ region. We consider several perturbative aspects related to the choice of the scale setting adopted in resummed calculations, and we assess their impact on the theoretical prediction both for the differential $p_T^{\ell\ell}$ spectrum and for the N^{3}LO fiducial cross section. For both quantities, we find the results obtained with the different setups to be compatible with each other within the quoted uncertainty, highlighting the robustness of the theoretical prediction. In all cases, the experimental LHC data for the $p_T^{\ell\ell}$ spectrum is well described by our calculation.

1 Introduction

The theoretical description of the Drell–Yan $p_T^{\ell\ell}$ spectrum is among the most challenging tasks in collider physics at present, due to the outstanding accuracy reached by the experimental measurements. In a recent article [1], we have presented the state of the art, N^{3}LO calculation of the fiducial Drell–Yan cross section and its leptonic distributions such as $p_T^{\ell\ell}$, also studying the effect of the inclusion of QCD resummation of large logarithms of $M_{\ell\ell}/p_T^{\ell\ell}$, with $M_{\ell\ell}$ being the Drell–Yan pair invariant mass. Our findings indicate that a first-principle calculation using perturbative QCD methods describes well the experimental data for the differential $p_T^{\ell\ell}$ distribution measured in the regime $M_{\ell\ell} \sim M_Z$, with the exception of the very small $p_T^{\ell\ell}$ region where a phenomenological modelling of non-perturbative effects is needed.

The high accuracy of the theoretical calculation requires a careful estimate of the associated uncertainties, which are below $\pm 5\%$ for $p_T^{\ell\ell} \lesssim 100\,\text{GeV}$. In these proceedings we briefly review the calculation of Ref. [1] and we discuss various sources of theoretical uncertainty that are relevant for the description of the Drell–Yan $p_T^{\ell\ell}$ spectrum. We focus our discussion on aspects particularly

† Speaker.

relevant in the $p_T^{\ell\ell} \lesssim 100\,\text{GeV}$ region: the resummation of logarithmic corrections and the matching of resummation with the fixed order prediction.

The prediction of Ref. [1] for the differential $p_T^{\ell\ell}$ spectrum is based on a combination of a resummed calculation at N^{3}LL (including constant terms up to $\mathcal{O}(\alpha_s^3)$) obtained with `RadISH`[2,3,4] with the NNLO calculation obtained with `NNLOJET`[5,6,7]. The formulation adopted in the `RadISH` code is based on a momentum-space formalism and does not introduce any modelling of non-perturbative effects. Instead, the Landau singularity is regularised by freezing the running of the strong coupling constant at scales of the order of 0.5 GeV and that of the parton distribution functions (PDFs) at the extraction scale of the set adopted, which in this case corresponds to 1.65 GeV [8]. We will comment further on the prescription used to freeze the PDFs below. This prescription leads to effects in the calculation in the first two bins of the $p_T^{\ell\ell}$ distribution where non perturbative (NP) dynamics becomes relevant. In this region a realistic modelling of NP corrections is therefore necessary.

In the following, we study the impact on the theoretical uncertainties of various sources of higher-order corrections, related to the central scale setting used in our predictions.

2 Computational setup

Throughout this note, we will consider proton–proton collisions at a centre-of-mass energy $\sqrt{s} = 13\,\text{TeV}$, and we adopt the `NNPDF4.0` parton densities [8] at NNLO with $\alpha_s(M_Z) = 0.118$, whose scale evolution is performed with `LHAPDF` [9] and `Hoppet` [10], correctly accounting for heavy-quark thresholds. We set the central factorisation and renormalisation scales to $\mu_F = \mu_R = \sqrt{{M_{\ell\ell}}^2 + {p_T^{\ell\ell}}^2}$. We adopt the G_μ scheme with the following EW parameters taken from the PDG [11]: $M_Z = 91.1876\,\text{GeV}$, $M_W = 80.379\,\text{GeV}$, $\Gamma_Z = 2.4952\,\text{GeV}$, $\Gamma_W = 2.085\,\text{GeV}$, and $G_F = 1.1663787 \times 10^{-5}\,\text{GeV}^{-2}$. We consider a fiducial volume [12] in which the leptonic invariant mass window is constrained to be $66\,\text{GeV} < M_{\ell\ell} < 116\,\text{GeV}$ and the lepton rapidities are confined to $|\eta^{\ell^\pm}| < 2.5$. The transverse momenta of the two leptons are required to satisfy $|\vec{p}_T^{\,\ell^\pm}| > 27\,\text{GeV}$.

3 Resummation scheme and scale setting for the $\mathcal{O}(\alpha_s^3)$ constant terms

We start by discussing the impact of the choice of the strong coupling scale in the $\mathcal{O}(\alpha_s^3)$ constant terms in the resummation formula. Here we deliberately use a very schematic and simplistic language to introduce how they arise in the resummed calculation. An appropriate discussion of these terms and their structure within the `RadISH` framework is reported in Ref. [13], where the scale setting adopted in Ref. [1] is discussed in detail. Schematically, one can parametrise the perturbative logarithmic counting for the resummed cumulative cross section considered here as

$$\mathcal{C}(\alpha_s(M_{\ell\ell}), \alpha_s(\mu)) \, \exp\{ \sum_{i=-1}^{2} \alpha_s^i \, h_{i+2}(\alpha_s L) + \dots \}, \tag{1}$$

where $\alpha_s \equiv \alpha_s(M_{\ell\ell})$ and L denotes the large logarithms which are resummed in the $p_T^{\ell\ell} \ll M_{\ell\ell}$ regime. The function $\mathcal{C}(\alpha_s(M_{\ell\ell}), \alpha_s(\mu))$ encodes constant contributions that survive in the $p_T^{\ell\ell} \to 0$ limit. It admits a perturbative expansion in powers of the strong coupling α_s, which is needed up to three loops ($\mathcal{O}(\alpha_s^3)$) [14,15,16,17] in order to achieve, together with the functions $h_i(\alpha_s L)$, the accuracy of the predictions of Ref. [1] in the regime $\alpha_s L \sim 1$ and $\alpha_s \ll 1$.

We first turn our focus on the scale of the coupling constant in the perturbative expansion of $\mathcal{C}(\alpha_s(M_{\ell\ell}), \alpha_s(\mu))$. At each order $\mathcal{O}(\alpha_s^i)$ this receives contributions both from terms evaluated at $\alpha_s^i(M_{\ell\ell})$ and from terms evaluated at $\alpha_s^i(\mu)$, where the scale $\mu \ll M_{\ell\ell}$ is of the order of the transverse momentum of the QCD radiation probed in the $p_T^{\ell\ell} \to 0$ limit. The precise value of this scale depends on the resummation formalism. Within `RadISH` this is set as $\mu \sim k_{t1}$, with k_{t1} being

the transverse momentum of the hardest initial-state radiation, while in an impact-parameter approach this is set as $\mu \sim 1/b$, with b being the impact parameter (see e.g. Refs. [18,19,20]). These two scales are of the same order and are related by a Bessel integral transform [3].

In a direct QCD formulation of $p_T^{\ell\ell}$ resummation, the separation of terms evaluated at $\alpha_s^i(M_{\ell\ell})$ and those evaluated at $\alpha_s^i(\mu)$ specifies the so-called *resummation scheme* [19], and only the combination of both factors in Eq. (1) is resummation-scheme invariant. More precisely, if we denote by $\mathcal{C}^{(i)}$ the $\mathcal{O}(\alpha_s^i)$ term of the perturbative expansion of $\mathcal{C}(\alpha_s(M_{\ell\ell}), \alpha_s(\mu))$, only the combination of $\mathcal{C}^{(i)}$ and $h_{i+2}(\alpha_s L)$ is resummation-scheme invariant. Consequently, a change in the renormalisation scale in the $\mathcal{O}(\alpha_s^3)$ constant terms $\mathcal{C}^{(3)}$ will affect the form of the correction $\alpha_s^3 h_5(\alpha_s L)$ in Eq. (1), which is a genuine N^{4}LL correction and hence beyond the perturbative accuracy of the calculation discussed here.

The prediction presented in Ref. [1] evaluates the $\mathcal{O}(\alpha_s^3)$ terms with $\alpha_s(M_{\ell\ell})$; it is however possible to evaluate the terms of hard-virtual origin in $\mathcal{C}^{(3)}$ at $\alpha_s(M_{\ell\ell})$, while those of soft and/or collinear origin are evaluated at $\mu \sim k_{t1} \ll M_{\ell\ell}$. The difference between the two prescriptions is, as explained above, subleading in the perturbative order of the calculation. As such, one expects it to be compatible within the quoted perturbative uncertainties.

A study of the difference between the two scale settings in the `RadISH`+`NNLOJET` prediction was presented in Ref. [13]. The difference between the two scale settings is shown in Fig. 1 (left), where the blue, hatched band represents our default setup used in Ref. [1], and the green, solid band shows the result with the constant terms of soft and/or collinear origin evaluated at the scale $\mu = k_{t1}$ (labelled with $\mu \neq M_{\ell\ell}$ in the plot) up to $\mathcal{O}(\alpha_s^3)$. The uncertainties are still estimated as outlined in Ref. [1]. In particular, this prescription includes a very conservative estimate of the matching uncertainty, which is obtained by taking the envelope of the uncertainty bands obtained with *four* different matching schemes, for a total of 36 variations (9 scale variations per scheme). This conservative approach is taken given the level of precision that is reached by the perturbative calculation. Fig. 1 shows that the change in the scale μ leads to a distortion of the spectrum in such a way that it becomes softer at small $p_T^{\ell\ell}$ and slightly harder for $p_T^{\ell\ell} > 10\,\text{GeV}$. The resulting distribution in Fig. 1 is still compatible with the data and with our default setup within uncertainties, in line with the fact that it corresponds to a subleading logarithmic correction. An exception is the region between $[20, 40]\,\text{GeV}$ where the central value of the green band lies outside the error band (blue) of our default setup, suggesting that one may adopt a slightly more conservative error estimate that includes the central curve of the green band in the envelope that defines the theory uncertainty.

4 Evolution of parton densities and freezing

We now briefly discuss how the freezing of the parton densities at the extraction scale of $1.65\,\text{GeV}$ [8] impacts our prediction. As an alternative prescription, instead of freezing the parton densities at $Q_0 = 1.65\,\text{GeV}$, we evolve backward from this scale down to $0.5\,\text{GeV}$ taking correctly into account the charm-quark mass threshold. This ensures that possible small artefacts related to the freezing of the parton densities are pushed to the very small $p_T^{\ell\ell}$ region. Fig. 1 (right) shows the comparison of the default setup of Ref. [1] to the prediction obtained with the above treatment of the parton distribution functions, that we label as *hybrid* in the plot. As it can be appreciated from the figure, the freezing only modifies the prediction for this setup at very small $p_T^{\ell\ell}$ values, in a way that is fully compatible with our estimate of the theory uncertainties.

5 The resummation scale

Finally, we discuss another relevant aspect in the scale setting used in the `RadISH` calculations, which concerns the value of the hard scale of the process, of the order of $M_{\ell\ell}$. This hard scale is set to $M_{\ell\ell}/2$ in the `RadISH` predictions of Ref. [1]. An associated variation of this perturbative

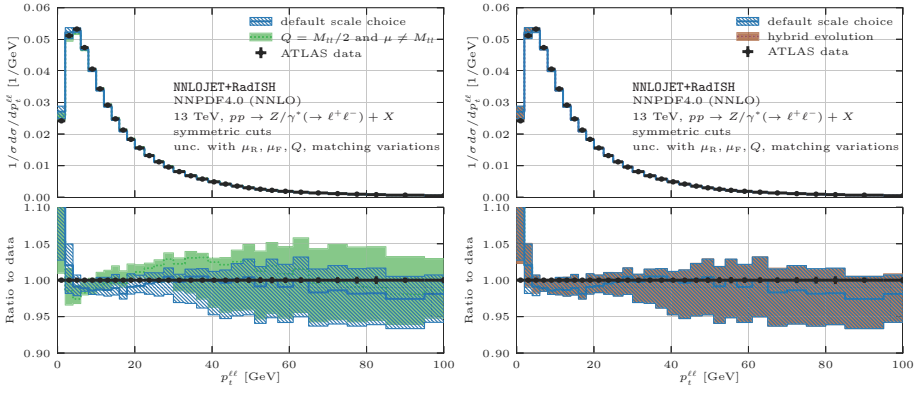

Figure 1 – Left panel: fiducial $p_T^{\ell\ell}$ distribution at N^{3}LO+N^{3}LL in the default scale setup of Ref. [1] (blue, hatched) and evaluating the $\mathcal{O}(\alpha_s^3)$ constant terms of soft and collinear origin at $\mu = k_{t1}$ (green, solid). See Ref. [13] for a more detailed discussion. Right panel: Fiducial $p_T^{\ell\ell}$ distribution at N^{3}LO+N^{3}LL in the default scale setup of Ref. [1] (blue, hatched) and using the hybrid evolution for the parton densities below the extraction scale (brown, solid).

scale (as well as of the other perturbative scales) is encoded in the estimate of the perturbative uncertainties. In the RadISH formalism, this scale enters in the form of a resummation scale Q. This can be introduced by decomposing the resummed logarithm L as [21,13]

$$L = \tilde{L} + \ln \frac{M_{\ell\ell}}{Q}\,, \tag{2}$$

and re-expanding L about $\tilde{L}$ while neglecting subleading (N^{4}LL) corrections. This is motivated by the fact that in the $p_T^{\ell\ell} \to 0$ limit one has $\tilde{L} \gg \ln \frac{M_{\ell\ell}}{Q}$. A variation of the scale Q (commonly by a factor of two about its central value) then probes the size of subleading logarithmic corrections in the uncertainty estimate. At the same time, the logarithm $\tilde{L}$ is switched off for $p_T^{\ell\ell} \gtrsim Q$ with a smooth deformation [21,13] that introduces power corrections of order $(p_T^{\ell\ell}/Q)^{p-1}$ (we choose the parameter $p = 6$) in the $p_T^{\ell\ell}$ differential distributions. These facilitate the matching of the resummed result to the fixed order calculation and appear only at subleading orders with respect to the nominal result, that is at $\mathcal{O}(\alpha_s^4)$. In this way, the scale Q also takes the role of the scale at which resummation effects are switched off in the $p_T^{\ell\ell}$ distribution. Choosing $Q = M_{\ell\ell}$ as a central scale implies that a variation of Q in the assessment of the theory uncertainty will induce residual resummation effects up to $p_T^{\ell\ell} \sim 2M_{\ell\ell}$, which is a rather high scale. For this reason, our default setup is to vary Q about its central value $M_{\ell\ell}/2$, above which QCD is well described by fixed-order perturbation theory.

Nevertheless, in the following we study the difference between the two scale settings. For this reason, in Fig. 2 we show the comparison between the RadISH+NNLOJET prediction using either $Q = M_{\ell\ell}/2$ (our default, given by the blue, hatched band) or $Q = M_{\ell\ell}$ (given by the red, solid band) as a central scale. In the latter, we also adopt the hybrid treatment of the evolution of parton distribution functions (PDFs) discussed above, to avoid any interplay between the PDFs freezing scale and the perturbative prediction in the small $p_T^{\ell\ell}$ region. The uncertainties in the red band of Fig. 2 are estimated as done in Ref. [13], by performing scale variations within three matching schemes [a] that ensure that the resummation is switched off at $p_T^{\ell\ell} \sim M_{\ell\ell}$. We observe that the prediction with $Q = M_{\ell\ell}$ as a central scale receives a shift in the upward (downward)

[a] In this case, due to the high resummation scale, we only consider the three matching schemes involving a matching factor (see Ref. [13]). The corresponding uncertainty thus consists of 27 variations.

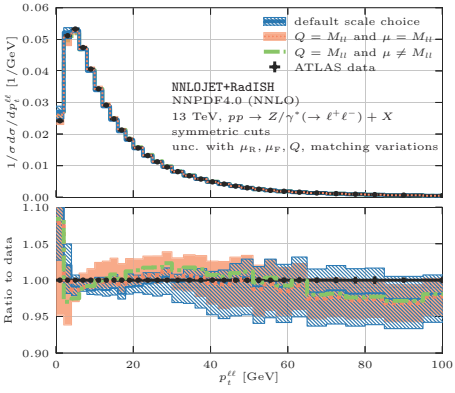

Figure 2 – Fiducial $p_T^{\ell\ell}$ distribution at N^{3}LO+N^{3}LL in the default scale setup of Ref. [1] (blue, hatched) and setting the central value of the resummation scale at $Q = M_{\ell\ell}$ (red, solid). The green-dashed curve indicates the central prediction with $Q = M_{\ell\ell}$ and $\mu \neq M_{\ell\ell}$.

direction for $p_T^{\ell\ell} > (<)\, 10\,\text{GeV}$. Moreover, the perturbative uncertainty grows with this different resummation scale, and the prediction remains compatible with the experimental data.

Finally, it is instructive to adopt the three modifications to our default setting discussed in this note together. That is, we use $\mu \neq M_{\ell\ell}$ as outlined in the previous section together with $Q = M_{\ell\ell}$ in our prediction. The result is displayed by the dot-dashed light-green line in Fig. 2, and it is entirely within the (red) uncertainty band of the $Q = M_{\ell\ell}$ result as one would expect from a subleading effect.

6 Impact on the fiducial cross section

As a last step, we also discuss the impact of the different scale setting discussed in this note on the fiducial cross section at N^{3}LO+N^{3}LL presented in Ref. [1]. This reference quotes $726.2(1.1)^{+1.07\%}_{-0.77\%}$ pb for the fiducial cross section within symmetric cuts, compatible with the N^{3}LO result of $722.9(1.1)^{+0.68\%}_{-1.09\%} \pm 0.9$ pb, computed in the same article. The central value of the N^{3}LO+N^{3}LL cross section obtained within the setup shown in the green band of Fig. 1 (left) (namely with $\mu \neq M_{\ell\ell}$) is 725.0(1.1) pb, while the central value corresponding to the red band of Fig. 2 is 723.8(1.1) pb. Both values are well within the scale uncertainty of the N^{3}LO+N^{3}LL calculation performed in Ref. [1], which confirms the robustness of this prediction for the fiducial cross section.

7 Conclusions

In these proceedings we have discussed the dependence of the `RadISH`+`NNLOJET` predictions of Ref. [1] upon different choices for the perturbative scale setting. We observed that all setups yield results which are compatible with each other within the quoted uncertainties. This indicates that the latter uncertainty is reliable, although a more conservative estimate could be envisaged by taking into account the spectrum of variations considered here. All of our predictions agree well with the experimental LHC data, possibly with the exclusion of the very small $p_T^{\ell\ell}$ region, which requires a careful assessment of non-perturbative effects.

We have also examined the impact of the different setups on the fiducial cross section at N^{3}LO+N^{3}LL, finding in all cases that the effect of the different scale choices is well within the perturbative uncertainty band obtained in Ref. [1], highlighting its robustness.

Acknowledgments

We thank the organisers of the 56$^{\text{th}}$ Rencontres de Moriond 2022. This work has received funding from the Deutsche Forschungsgemeinschaft (DFG, German Research Foundation) under

grant 396021762-TRR 257, from the Swiss National Science Foundation (SNF) under contracts PZ00P2_201878, 200020_188464 and 200020_204200, from the UK Science and Technology Facilities Council (STFC) through grant ST/T001011/1, from the Italian Ministry of University and Research (MIUR) through grant PRIN 20172LNEEZ, and from the European Research Council (ERC) under the European Union's Horizon 2020 research and innovation programme grant agreement 101019620 (ERC Advanced Grant TOPUP).

References

1. X. Chen, T. Gehrmann, E. W. N. Glover, A. Huss, P. Monni, E. Re, L. Rottoli, and P. Torrielli. Third-Order Fiducial Predictions for Drell-Yan Production at the LHC. *Phys. Rev. Lett.*, 128(25):252001, 2022.
2. Pier Francesco Monni, Emanuele Re, and Paolo Torrielli. Higgs Transverse-Momentum Resummation in Direct Space. *Phys. Rev. Lett.*, 116(24):242001, 2016.
3. Wojciech Bizon, Pier Francesco Monni, Emanuele Re, Luca Rottoli, and Paolo Torrielli. Momentum-space resummation for transverse observables and the Higgs $p_\perp$ at N^{3}LL+NNLO. *JHEP*, 02:108, 2018.
4. Pier Francesco Monni, Luca Rottoli, and Paolo Torrielli. Higgs transverse momentum with a jet veto: a double-differential resummation. *Phys. Rev. Lett.*, 124(25):252001, 2020.
5. A. Gehrmann-De Ridder, T. Gehrmann, E. W. N. Glover, A. Huss, and T. A. Morgan. Precise QCD predictions for the production of a Z boson in association with a hadronic jet. *Phys. Rev. Lett.*, 117(2):022001, 2016.
6. Aude Gehrmann-De Ridder, T. Gehrmann, E. W. N. Glover, A. Huss, and T. A. Morgan. The NNLO QCD corrections to Z boson production at large transverse momentum. *JHEP*, 07:133, 2016.
7. A. Gehrmann-De Ridder, T. Gehrmann, E. W. N. Glover, A. Huss, and T. A. Morgan. NNLO QCD corrections for Drell-Yan p_T^Z and ϕ^* observables at the LHC. *JHEP*, 11:094, 2016. [Erratum: JHEP 10, 126 (2018)].
8. Richard D. Ball et al. The Path to Proton Structure at One-Percent Accuracy. 9 2021.
9. Andy Buckley, James Ferrando, Stephen Lloyd, Karl Nordström, Ben Page, Martin Rüfenacht, Marek Schönherr, and Graeme Watt. LHAPDF6: parton density access in the LHC precision era. *Eur. Phys. J. C*, 75:132, 2015.
10. Gavin P. Salam and Juan Rojo. A Higher Order Perturbative Parton Evolution Toolkit (HOPPET). *Comput. Phys. Commun.*, 180:120–156, 2009.
11. M. Tanabashi et al. Review of Particle Physics. *Phys. Rev. D*, 98(3):030001, 2018.
12. Georges Aad et al. Measurement of the transverse momentum distribution of Drell–Yan lepton pairs in proton–proton collisions at $\sqrt{s} = 13$ TeV with the ATLAS detector. *Eur. Phys. J. C*, 80(7):616, 2020.
13. Emanuele Re, Luca Rottoli, and Paolo Torrielli. Fiducial Higgs and Drell-Yan distributions at N^{3}LL$'$+NNLO with RadISH. *JHEP*, 09:108, 2021.
14. T. Gehrmann, E. W. N. Glover, T. Huber, N. Ikizlerli, and C. Studerus. Calculation of the quark and gluon form factors to three loops in QCD. *JHEP*, 06:094, 2010.
15. Ye Li and Hua Xing Zhu. Bootstrapping Rapidity Anomalous Dimensions for Transverse-Momentum Resummation. *Phys. Rev. Lett.*, 118(2):022004, 2017.
16. Ming-xing Luo, Tong-Zhi Yang, Hua Xing Zhu, and Yu Jiao Zhu. Quark Transverse Parton Distribution at the Next-to-Next-to-Next-to-Leading Order. *Phys. Rev. Lett.*, 124(9):092001, 2020.
17. Markus A. Ebert, Bernhard Mistlberger, and Gherardo Vita. Transverse momentum dependent PDFs at N^{3}LO. *JHEP*, 09:146, 2020.
18. John C. Collins, Davison E. Soper, and George F. Sterman. Transverse Momentum Distribution in Drell-Yan Pair and W and Z Boson Production. *Nucl. Phys. B*, 250:199–224, 1985.
19. Stefano Catani, Daniel de Florian, and Massimiliano Grazzini. Universality of nonleading logarithmic contributions in transverse momentum distributions. *Nucl. Phys. B*, 596:299–312, 2001.
20. Thomas Becher and Matthias Neubert. Drell-Yan Production at Small q_T, Transverse Parton Distributions and the Collinear Anomaly. *Eur. Phys. J. C*, 71:1665, 2011.
21. Wojciech Bizoń, Xuan Chen, Aude Gehrmann-De Ridder, Thomas Gehrmann, Nigel Glover, Alexander Huss, Pier Francesco Monni, Emanuele Re, Luca Rottoli, and Paolo Torrielli. Fiducial distributions in Higgs and Drell-Yan production at N^{3}LL+NNLO. *JHEP*, 12:132, 2018.